A Hysteresis ON-OFF Control Method of Inductive Power Transfer Systems with Low Output Ripples and Fast Transient Responses

[*]Jiayu Zhou, [†]Giuseppe Guidi, [#]Shuxin Chen, [#]Yi Tang, and [*,†]Jon Are Suul
[*]Department of Engineering Cybernetics, Norwegian University of Science and Technology, Trondheim, Norway
[†]SINTEF Energy Research, Trondheim, Norway
[#]School of Electrical and Electronic Engineering, Nanyang Technological University, Singapore
Jiayu.zhou@ntnu.no, giuseppe.guidi@sintef.no, chen1095@e.ntu.edu.sg, yitang@ntu.edu.sg, Jon.A.Suul@ntnu.no

***Abstract*—This paper proposes a hysteresis ON-OFF control method for inductive power transfer (IPT) systems with low output ripples and fast transient responses. System power is regulated by skipping pulses, thus achieving zero voltage switching over the full operating range. Moreover, each switching state is determined by a hysteresis comparator operating on the measured power. This prevents the skipped pulses from exciting poorly damped oscillations. The dynamic behavior of IPT systems with the hysteresis ON-OFF control method is excellent because the controlled state of the system is directly adjusted in every half cycle. The effectiveness and feasibility of the proposed method are validated by simulations and experimental results from a small-scale laboratory prototype.**

Keywords—Dynamic behavior, Hysteresis ON/OFF control, Inductive power transfer, Ripple suppression

I. Introduction

Wireless inductive power transfer (IPT) using magnetic resonant coupling is being increasingly utilized for a wide range of applications where physical connection is inconvenient or impossible, such as wireless power supplies/chargers for electric vehicles [1], biomedical implants [2], and marine transports [3]. Achieving soft switching and ensuring dynamic response in the full range of expected operating conditions is very important for IPT systems. However, this can be challenging to achieve under large variations in load and magnetic coupling.

In high-power inductive battery charging applications, the series-series (SS) compensated topology with a diode rectifier on the pickup side is usually found most suited in term of system cost, complexity, and power density [3]. However, the degrees of freedom in the control of such systems are limited, and include only the operating frequency and the sending voltage value. For variable frequency control methods, instability issues may be posed in dynamic response due to the bifurcation phenomenon for traditional frequency control methods [4]. For the sub-resonant frequency control, power capability is limited in pursuit of high efficiency and minimum voltampere rating [5]. For voltage control methods, phase shift modulation (PSM) is the most common method, which usually results in hard switching in systems with highly variable coupling and output power.

Recently, some pulse skipping methods based on voltage control are proposed for IPT systems, such as pulse density modulation (PDM) [6]-[8] and ON-OFF keying (OOK) modulation [9]. These methods adjust the sending voltage by skipping pulses to achieve output power regulation on the system, and can always achieve zero voltage switching (ZVS) under output power variations. However, IPT systems with constant voltage load (CVL) and PDM can experience large current/power oscillations due to poor system damping [10]. The PDM patterns are modified in [11] to reduce ripples under fixed working conditions, which is difficult to guarantee that large ripples can be avoided in a wide variation in coupling and output power. Moreover, an active damping method is proposed in [10] to suppress current/power ripples but introduce PSM for a small number of cycles resulting in loss of ZVS. In [9], an OOK modulation is proposed to achieve high efficiency in the whole operating range, but large current/power oscillation cannot be avoided due to the system switching between long-time OFF states and full load. Therefore, the above methods are not suitable for high-power applications.

In this paper, a hysteresis ON-OFF control method is proposed to achieve high efficiency, low ripples, and fast transient response within the full required operating range. In IPT systems with the hysteresis ON-OFF control, the system power is calculated in real time and compared with the power reference value to determine the next switching state. It is worth noting that the input power is regulated to avoid the need for dual-side communication, and to prevent that delayed output power/current ripples appear in the feedback signal. Compared with the previously mentioned pulse skipping methods [6]-[11], the hysteresis control method has upper and lower limits of the controlled state, which can directly suppress the current/power oscillations of the system. Moreover, the dynamic behavior of the system is significantly improved, because the system can directly judge and control the system power every switching cycle. Specific feedback loops and hysteresis bands of the system are designed in detail in this paper. The validity of the hysteresis ON-OFF control method for IPT systems is verified by simulations and experimental results obtained from a laboratory prototype.

This work was conducted within the project "Ultra-high power density wireless charging for maritime applications," supported by the Research Council of Norway under Project number 294871 and Singapore Maritime Institute under Project SMI-2019-MA-02.

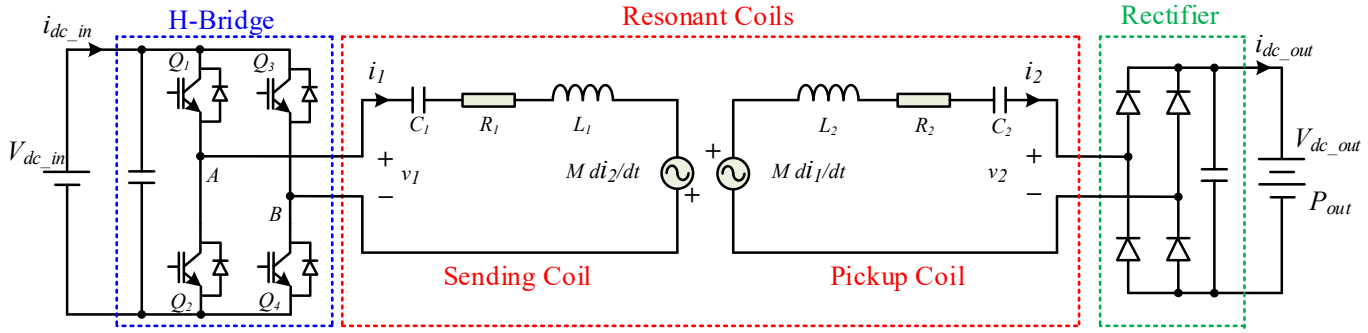

Fig.1. The SS-compensated IPT system with constant voltage load.

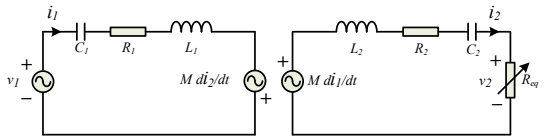

Fig.2. Equivalent circuit of SS-compensated IPT system using harmonic approximation and equivalent load resistance.

II. System Design and Basic Characteristics of SS-Compensated IPT Systems with CVL

The circuit of a typical SS-compensated IPT system with CVL is shown in Fig. 1, where v_1 (v_2), i_1 (i_2), L_1 (L_2), C_1 (C_2), and R_1 (R_2) are the sending (pickup) voltage, current, inductance, capacitance, and series-equivalent resistances, respectively, and M is the mutual inductance. A diode rectifier is applied at the pickup side to reduce system cost and complexity. Moreover, the system output is directly connected to a battery which can be modelled as a CVL. Based on the first harmonic approximation, the input (output) terminal voltage v_1 (v_2) can be assumed to be a sinusoidal signal. To facilitate the discussion of steady-state results, the diode rectifier and CVL can be equivalent to a resistance R_{eq}. In this case, the equivalent circuit of the IPT system using harmonic approximation and equivalent load resistance is obtained as shown in Fig. 2. It is worth noting that the equivalent load varies with the output power. The maximum coil efficiency of the IPT system shown in Fig. 1 is given by [1]:

$$\eta_{\max} = \frac{k^2 Q^2}{(1+\sqrt{1+k^2Q^2})^2} \tag{1}$$

where the quality factor Q and the coupling coefficient k are expressed as:

$$k = \frac{M}{\sqrt{L_1 L_2}} \tag{2}$$

$$Q = \sqrt{Q_1 \cdot Q_2} = \sqrt{\frac{\omega_0 L_1}{R_1}\frac{\omega_0 L_2}{R_2}} \tag{3}$$

The maximum efficiency is only achieved when the conventional SS-compensated IPT system is operated at resonance frequency ω_0 and satisfies the following equation:

$$R_{eq\_opt} = \frac{\omega_0 \cdot L_2}{Q_2}\sqrt{1+k^2Q^2} \tag{4}$$

In this expression, $(kQ)^2 >> 1$, implying that 1 can be neglected. Moreover, the material of the coils on the sending side and the pickup side are the same and the values of Q and Q_2 are very close. Therefore, the equation (4) can be simplified as:

$$R_{eq\_opt} \approx \omega_0 \cdot L_2 \cdot k \tag{5}$$

Assuming an ideal system with lossless components, the output power of the system operating at the resonance frequency can be calculated as:

$$P_{out} = \frac{V_1 \cdot V_2}{\omega_0 \cdot M} \tag{6}$$

In this case, the equivalent resistance on the pickup side can be expressed as:

$$R_{eq} = \frac{V_2^2}{P_{out}} = \frac{\omega_0 \cdot M \cdot V_2}{V_1} \tag{7}$$

According to equations (5) and (7), the condition that R_{eq} is equal to R_{eq_opt} for achieving optimal efficiency can be calculated as:

$$\sqrt{\frac{L_1}{L_2}} \cdot \frac{V_2}{V_1} = 1 \tag{8}$$

Since a diode rectifier is used on the pickup side to connect the CVL, the magnitude of v_2 will remain constant and is expressed as:

$$V_2 = \frac{2\sqrt{2}}{\pi} \cdot V_{dc,out} \tag{9}$$

However, V_1 is to be controller to regulate system power, so systems with the diode rectifier cannot always track optimal efficiency as shown in (1). In this case, the system is designed according to equation (8) at the rated operating point. Moreover, the system is expected to avoid hard switching over the full operating range, so the resonance frequency of the pickup side can be designed to be slightly higher than that of the sending side to achieve ZVS. The detuning factor x_c is introduced and designed to be slightly larger than 1 [5]:

$$x_c = \frac{C_1 \cdot L_1}{C_2 \cdot L_2} \tag{10}$$

TABLE I
Parameters of the IPT-System

General parameters	Values
Nominal power, P_0	150 W
Nominal receiving voltage, V_2	50 V
Coupling coefficient, k	0.2-0.3
pickup coil resonant frequency, f_r	85.0 kHz
Self-inductance, L_1, L_2	125, 125 μH
Quality factor, Q_1, Q_2	350, 350
Detuning factor, x_c	1.03

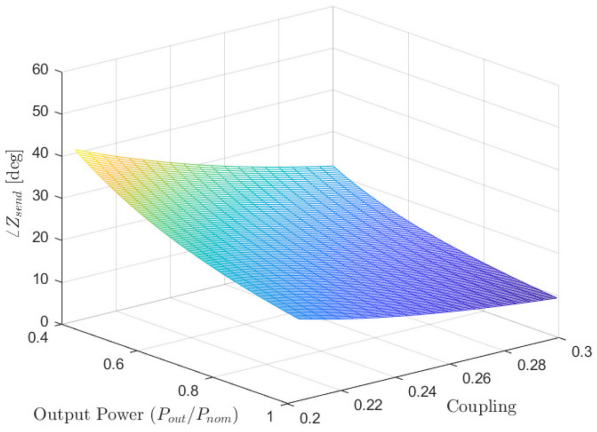

Fig.3. The impedance angle of the IPT system with different operating points.

It is worth noting that the x_c is close to 1 and will not significantly affect the conclusions from equations (1) - (8). By using the parameters provided in Table I, the input impedance angles of the IPT system at different operating points can be obtained, as shown in Fig. 3. It can be found that the input impedance of the system is inductive in the full operating range. In this case, pulse skipping modulations, such as PDM and OOK, can be used to constrain the system power by skipping pulses. Therefore, a full range of ZVS can be achieved. However, there are large current/power ripples at certain densities in CVL systems due to the extremely low damping of modes that can be excited by skipping pulses. Moreover, dynamic performance of the system is difficult to guarantee over a wide range of coupling changes. In this paper, a hysteresis ON-OFF modulation method is proposed to avoid hard switching, while allowing the system to maintain low output ripples and fast transient responses.

III. The Hysteresis ON-OFF Modulation Method Design and Implementation

A. Principle of the Hysteresis ON-OFF Modulation

In IPT systems with established pulse skipping methods, the system power is usually regulated by adjusting a modulation density [6]-[11]. Moreover, the timing of the skipped pulse is determined by the feedback modulation density and inherent modulation modes. In this case, the real-time state of the system does not directly determine switching states. Therefore, in case of systems with poorly damped modes caused by CVL characteristics the skipped pulses might cause large oscillations that are difficult to eliminate [10]. To overcome the above problems, a hysteresis ON-OFF modulation method for IPT systems is proposed in this paper.

Fig. 4 shows the proposed hysteresis ON-OFF control strategy for IPT systems. The duty cycle of the input signal is 50%, and the pulse frequency is the resonance frequency of the pickup side. A hysteresis comparator is used to determine the ON or OFF states of switches by comparing the power reference with the real-time system power. Moreover, the hysteresis comparator is triggered by the rising and falling edges of the input signal. Therefore, each switching state is determined by the real-time power of the system. In this case, a low hysteresis band can directly limit the powers ripple of the system. An

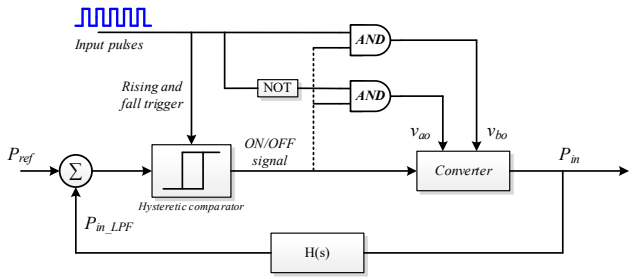

Fig. 4. The proposed hysteresis ON-OFF control method.

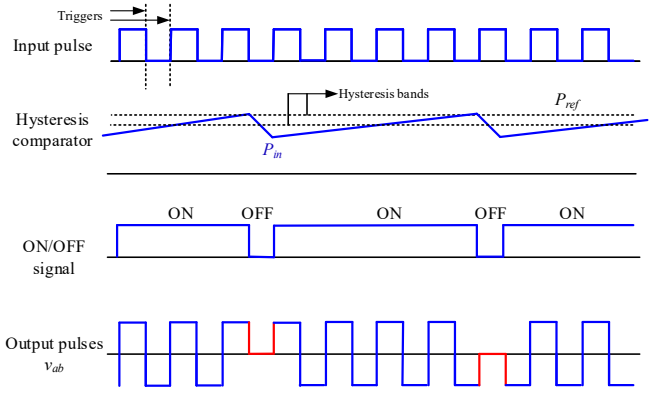

Fig. 5. Waveforms of the hysteresis ON-OFF modulation.

example of waveforms of the hysteresis ON-OFF modulation is given in Fig. 5. When the real-time power of the system is lower than the lower limit of the hysteresis band, switches of the converter are in the ON states, resulting in the continuous increase of the real-time power of the system. The switching states of the converter does not switch to OFF states until the real-time power is higher than the upper limit of the hysteresis band. It is worth noting that the ON/OFF signals are switched only at the triggered moments, which is why the P_{in} may be much lower than the low hysteresis comparator value before switching to the ON signal. The system power is therefore limited around the power reference.

B. Discussion of Power Feedback Signal

In IPT systems with CVL, the output power is usually regulated to control the system, which however requires dual-side communication in the closed-loop control. High-frequency real-time data transmission is sensitive to interference and communication speed, which poses the risk of transmission failure or even system instability. Moreover, the sending current/power ripples will always be caused by the pulse skipping, which further results in the output power ripples. In this case, the oscillation of the output power is delayed compared to the sending side. To suppress the power oscillation from the root cause, the input system power should be used for power regulation. Therefore, the output power of the system is estimated by input power and other known parameters. The output power P_{out} can be calculated as:

$$P_{out} = P_{in} + P_{Coils} + P_{Con\_D} \tag{11}$$

where P_{in} is the input power of the sending side. P_{Coils} is the loss of coils and P_{Con_D} is the total losses of the diode rectifier. P_{Coils} can be obtained by:

$$P_{Coils} = I_1^2 R_1 + I_2^2 R_2 \tag{12}$$

The losses of the diode rectifier mainly considers the conduction loss as shown below:

$$P_{Con\_D} = 2I_2^2 R_{diod\text{-}on} + \frac{4\sqrt{2}}{\pi} V_T I_2 \tag{13}$$

where V_T and $R_{diod\text{-}on}$ are the threshold voltage and the equivalent on-state resistance of the rectifier diode, respectively.

In IPT systems with CVL, the pickup current can be estimated from the input power:

$$I_2 \approx \frac{\pi}{2\sqrt{2}} \frac{P_{ref}}{V_{dc\_out}} \tag{14}$$

Therefore, the output power of the system can be estimated by equations (11)-(14) simultaneously:

$$P_{out} \approx P_{in} - I_1^2 R_1 - 2\frac{V_T P_{ref}}{V_{dc\_out}} - \frac{\pi^2}{8}\frac{P_{ref}^2}{V_{dc\_out}^2}(R_2 + 2R_{diod-on}) \tag{15}$$

In this case, the input power instead of the output power is used in the control to avoid dual-side communication and oscillation delays in the closed loop system.

C. Design of the Feedback Loop and Hysteresis Bands

In IPT systems with the hysteresis ON-OFF control method, each switching state of the system is determined by a real-time feedback power and the hysteresis comparator. Therefore, the design of the feedback loop and hysteresis bands needs to be discussed in detail. The input power during each switching state of the system is:

$$P_{in} = V_1 \cdot I_1 \tag{16}$$

The real-time value of V_1 at different switch states:

$$V_1 = \begin{cases} \frac{2\sqrt{2}}{\pi} \cdot V_{dc\_in} & ON\ states \\ 0 & OFF\ states \end{cases} \tag{17}$$

I_1 also fluctuates due to switching between ON and OFF states, which is limited by the hysteresis band. Compared with the fluctuation of V_1, the sending current fluctuation is small and is kept around the reference value. It can be found from equations (16) and (17) that the fluctuation of P_{in} is very large. In this case, a low hysteresis band cannot be set to guarantee a small error between the real-time system power and the power reference. Therefore, a low-pass filter (LPF) is used in the feedback control loop:

$$H(s) = \frac{1}{1 + T_f \cdot s} \tag{18}$$

where T_f is the time constant. In the discrete system, the filtered real-time power P_{in_LPF} can be calculated as:

$$P_{in\_LPF}(k) = q \cdot P_{in}(k) + (1-q) \cdot P_{in\_LPF}(k-1) \tag{19}$$

where $P_{in\_LPF}(k)$ and $P_{in\_LPF}(k\text{-}1)$ are the filtered power at the k^{th} and $(k+1)^{th}$ sampling instants. The filter coefficient q can be expressed as:

$$q = \frac{T_s}{T_f + T_s} \tag{20}$$

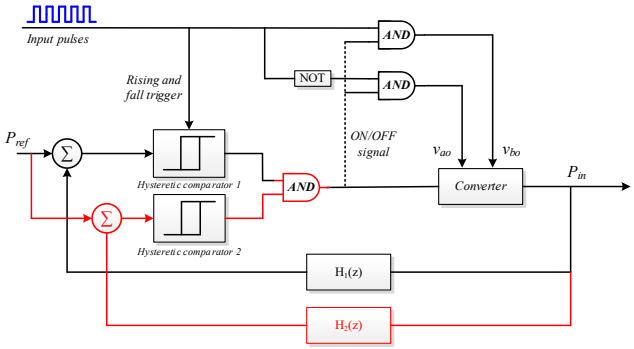

Fig. 6. The proposed hysteresis ON-OFF control method with a monitoring loop.

where T_s is the sampling period. Moreover, equation (19) can be written as:

$$P_{in\_LPF}(k) = P_{in\_LPF}(k-1) + \underbrace{q \cdot (P_{in}(k) - P_{in\_LPF}(k-1))}_{P_{ripple}} \tag{21}$$

From the above equation, the ripples of the filtered power P_{ripple} can be obtained. In general, the $P_{in\text{-}LPF}$ should converge to a value close to or approximately equal to by P_{ref} in a closed-loop system. Therefore, the main fluctuation of P_{in_LPF} comes from $P_{in}(k)$ due to the system switching between ON and OFF states. When ignoring the fluctuation of the sending current, the ripple of the filtered power per half cycle during ON states can be calculated as:

$$P_{ripple\_ON} \le q \cdot (P_{full} - P_{ref}) \tag{22}$$

where P_{full} is the power of the system in the full ON states. Similarly, the ripple of the filtered power per half cycle during OFF states can be obtained as:

$$P_{ripple\_OFF} \approx -q \cdot P_{ref} \tag{23}$$

To reduce the steady-state errors in closed-loop control, the hysteresis bands should be narrow, which are set to be $\pm$0.15W (0.1% of rated power) in this paper. To keep ripples per half cycle of the system close to the hysteresis bands in most cases, the filter coefficient q can be set to 0.01. In this case, the cutoff frequency of the feedback loop is about 1% of the switching frequency.

D. The Monitoring Loop

To reduce the steady-state errors by setting the small hysteresis bands, the cutoff frequency of the LPF of the control loop should also be low, which affect the dynamic behavior of the system. More importantly, the real-time states of the system in the dynamic process are not within the monitoring, and wrong decisions may be made on switching states. Therefore, a monitoring loop is added, as shown in Fig.6 marked in red line. Compared with the control loop, the cutoff frequency of the LPF in the monitoring loop is increased tenfold, and the corresponding hysteresis bands are also expanded tenfold. Therefore, the dynamic response performance of the system will be better, and the system status will be monitored quickly to ensure stability.

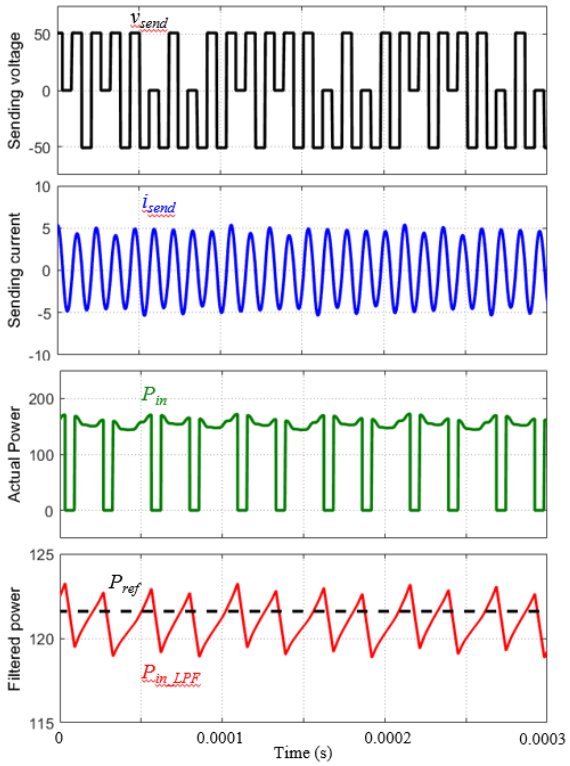

Fig. 7. Simulation results of the IPT system with the hysteresis ON-OFF modulation, operating at 0.8 P_{nom}.

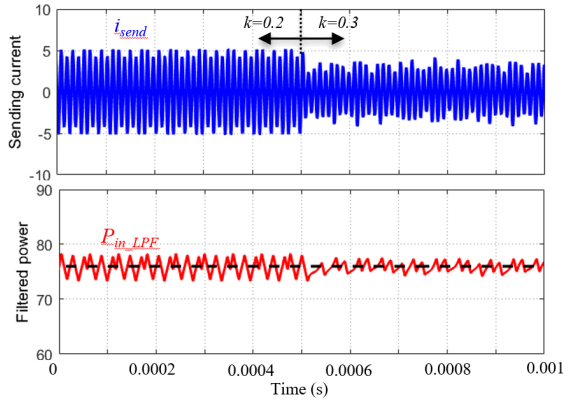

Fig. 8. Dynamic performance when coupling steps from 0.2 to 0.3.

IV. Simulation Results

To verify the effectiveness of the coordinated voltage-frequency control for SS-compensated IPT systems, a MATLAB/Simulink model is implemented. The system specifications are listed in Table I.

Fig. 7 shows the results for the IPT system with the hysteresis ON-OFF control method at 0.8 P_{nom}. As expected, the system always achieves ZVS. Although the actual input power of the system P_{in} fluctuates greatly, the filtered power P_{in_LPF} fluctuates around the power reference value. When P_{in_LPF} is lower than P_{ref}, switch states are ON. In this case, P_{in_LPF} continues to increase until it is above the power reference and switches to OFF states. It can be found that the system frequently switches between ON and OFF states, but the fluctuation of the filtered power and the sending current of the system is small.

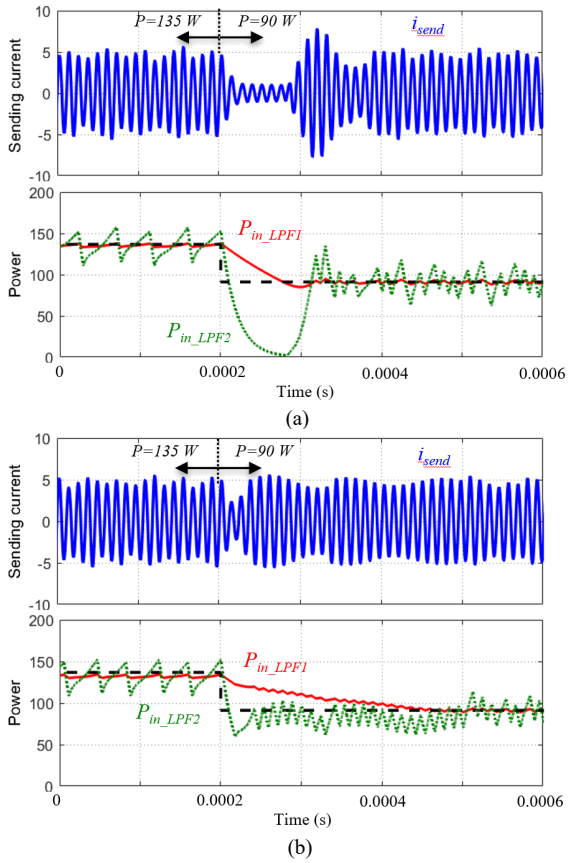

Fig. 9. Dynamic performance when the power reference value changes from 0.9 P_{nom} to 0.6 P_{nom}. (a) without the monitoring loop; (b) with the monitoring loop.

The dynamic results of the system with the hysteresis ON-OFF modulation are shown in Fig.8 and Fig. 9. When the coupling abruptly changes from 0.2 to 0.3, the system reaches a new steady state within a few switching cycles, as shown in Fig.8. Moreover, the sending current and filtered input power are also very stable without overshoot. Therefore, the proposed method is well suited for IPT applications where the coupling changes frequently, such as dynamic IPT systems for electric vehicles or marine applications. When the system power reference value is changed from 0.9 P_{nom} to 0.6 P_{nom}, the system performance is shown in Fig. 9. The red line represents the filtered power of the control loop, while the green dotted line is the filtered power value of the monitoring loop. It can be found that the system without the monitoring loop may operate in OFF states for a long time when P_{ref} drops momentarily, because the control bandwidth of the control loop is too low. In this case, the sending current may also overshoot, as shown in Fig. 9(a). When the monitoring loop is introduced into the system, the system will quickly operate around the new power reference value, as shown in Fig. 9(b). In this case, the error is relatively large before 0.0005s, which will not be suppressed until the filtered power P_{in_LPF1} of the control loop is also near the power reference. Therefore, the introduction of the

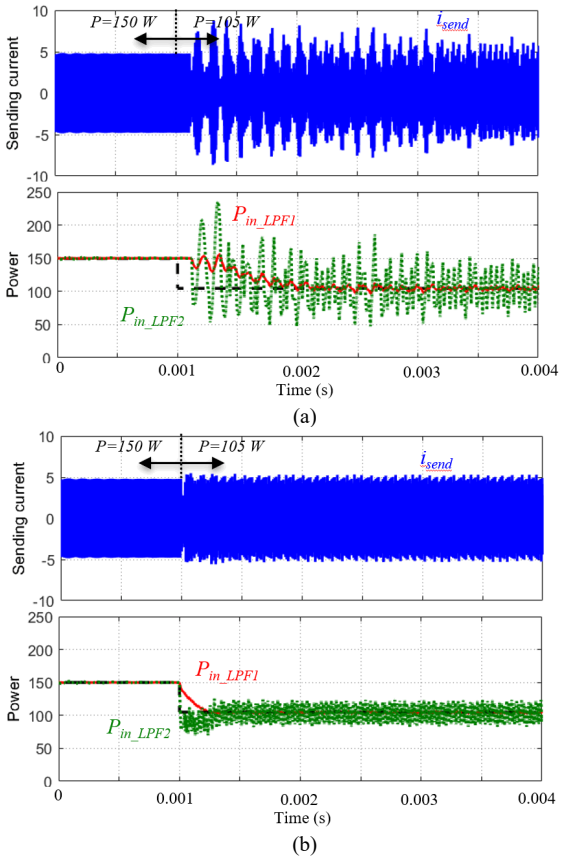

Fig. 10. Comparison of system performance between the IPT system with (a) PDM based on delta-sigma modulator; (b) the hysteresis ON-OFF modulation.

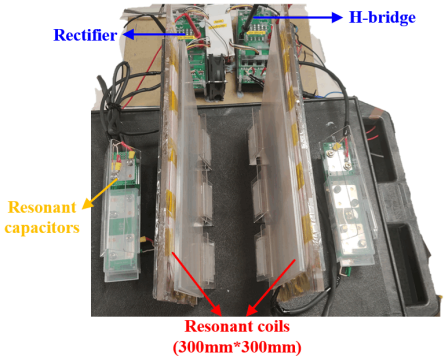

Fig. 11. Experimental setup of the IPT system.

monitoring loop avoids the misjudgment of switching states and the potential overshoot of the sending current.

In general, the modulation waveforms of the hysteresis ON-OFF method are similar to PDM in that they are frequently skipping pulses to regulate system power. However, the IPT system with the hysteresis ON-OFF method uses real-time power to determine the next switching state in every half cycle, thereby avoiding large current/power fluctuations. To judge the difference between these two methods more intuitively, the IPT system with PDM and the hysteresis control method are compared, as shown in Fig. 10. It can be found that the system with PDM has large sending current oscillations, because the frequency of the skipping pulses in the dynamic process may

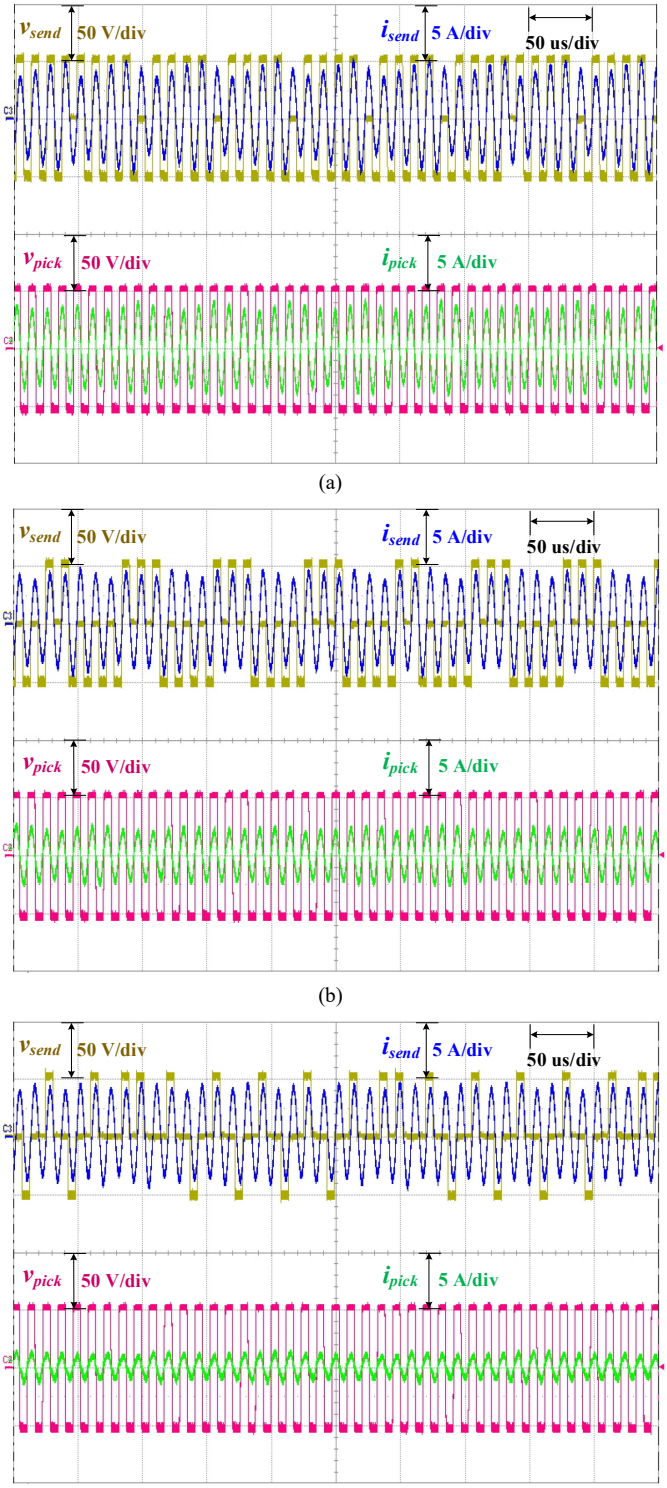

Fig.12. Experimental results of the system with the hysteresis ON-OFF modulation at (a) 0.9 P_{nom}; (b) 0.6 P_{nom}; (c) 0.3 P_{nom}.

be close to the natural frequency of the system [10]. The system with PDM reaches a new steady state at about 0.003s, and the current/power ripples are much smaller than that in the dynamic process. Fig. 10(b) shows the results of the IPT system with the proposed hysteresis control method under the same conditions. It can be found that the system is completely in the new steady

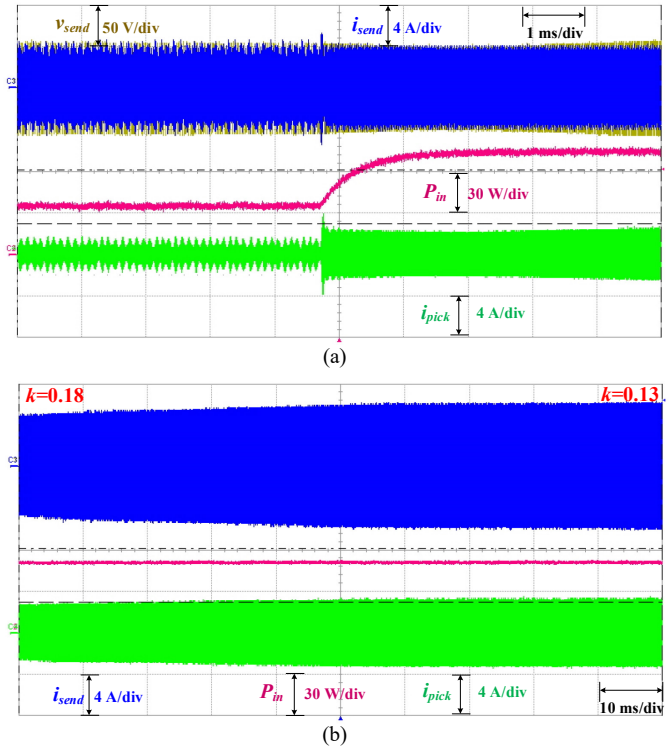

Fig. 13. The dynamic behavior of the system with the hysteresis ON-OFF control. (a) power steps from 35W to 75 W. (b) coupling changes from 0.18 to 0.13.

state at 0.0012s, and there are no large current/power oscillations in the dynamic process. Moreover, the current/power ripples of the system with the hysteresis control at steady states are also slightly smaller than that of the system with PDM.

V. Experimental Results

To further prove the results from the analysis and simulations, experiments are conducted with a laboratory prototype as shown in Fig. 11, designed with parameters listed in Table I. In the experiments, the input/output DC voltages were set to 50 V. Moreover, the sampling frequency of the system is twice the switching frequency, so that each switching action can be controlled.

Fig. 12 shows the experimental results of the system operating at different powers. It can be found that the system has always achieved ZVS. Moreover, the system regulates power by skipping pulses and always maintains low current ripples.

As for the dynamic response of the system, Fig. 13(a) shows the system performance when the system power is abruptly changed from 35W to 75W. It can be found that the sending/pickup current reaches a steady state instantaneously. The filter power of the system also tracks the reference power within 2ms. Fig. 13(b) shows the system dynamic performance when the system coupling changes in real time. It can be found that the sending current increases as the coupling decreases. It is worth noting that the system power remains stable and does not fluctuate with coupling changes. This also proves that the system with the hysteresis ON-OFF control has excellent dynamic performance, which is very suitable for IPT applications where coupling changes in real time.

VI. Conclusion

In this paper, a hysteresis ON-OFF control method for IPT systems is proposed to achieve full-range soft switching, maintain low current/power ripples, and ensure fast dynamic responses. In the proposed method, modulation pulses are skipped by comparing the power reference and real-time power value to regulate system power. The current/power ripples are suppressed by setting a small hysteresis band and a designed feedback loop. A monitoring loop is also introduced to the system to ensure high control bandwidth and system stability. Moreover, the dynamic behavior of IPT systems with the proposed method is excellent, which is well suited for systems with highly variable coupling and output power. Simulations and experimental results demonstrate the feasibility of the proposed method.

References

[1] S. Li and C. C. Mi, "Wireless power transfer for electric vehicle applications," *IEEE J. Emerg. Sel. Topics Power Electron*., vol. 3, no. 1, pp. 4–17, Mar. 2015.

[2] J. G. Bum *et al*., "An energy transmission system for an artificial heart suing leakage inductance compensation of transcutaneous transformer," *IEEE Trans. Power Electron.*, vol.13, no.6, pp. 1013-1022, Nov. 1998.

[3] G. Guidi, J. A. Suul, F. Jenset, and I. Sorfonn, "Wireless charging for ships: high-power inductive charging for battery electric and plug-in hybrid vessels," *IEEE Electr. Mag.*, vol. 5, no. 3, pp. 22–32, 2017.

[4] C. S. Wang, G. A. Covic, and O. H. Stielau, "Power transfer capability and bifurcation phenomena of loosely coupled inductive power transfer systems," *IEEE Trans. Ind. Electron.*, vol. 51, no. 1, pp. 148–157, Feb. 2004.

[5] G. Guidi and J. A. Suul, "Minimizing converter requirements of inductive power transfer systems with constant voltage load and variable coupling conditions," *IEEE Transactions on Industrial Electronics*, vol. 63, no. 11, pp. 6835–6844, Nov 2016.

[6] H. Li, J. Fang, S. Chen, K. Wang, and Y. Tang, "Pulse density modulation for maximum efficiency point tracking of wireless power transfer systems," *IEEE Trans. Power Electron.,* vol. 33, no. 6, pp. 5492–5501, Jun. 2018.

[7] V. Esteve, J. Jordán, E. Sanchis-Kilders, et al. "Enhanced Pulse-Density-Modulated Power Control for High-Frequency Induction Heating Inverters." IEEE Transactions on Industrial Electronics, vol. 62, no. 11, pp.6905-6914, Nov. 2015.

[8] H. Li, S. Chen, J. Fang, Y. Tang and M. A. de Rooij, "A low-subharmonic full-range and rapid pulse density modulation strategy for ZVS full-bridge converters", IEEE Trans. Power Electron., vol. 34, no. 9, pp. 8871-8881, Sep. 2019.

[9] W. Zhong and S. Y. R. Hui, "Maximum energy efficiency operation of series-series resonant wireless power transfer systems using on-off keying modulation," *IEEE Trans. Power Electron*., vol. 33, no. 4, pp. 3595–3603, Apr. 2018.

[10] J. Zhou, G. Guidi, K. Ljøkelsøy, J. A. Suul, "Analysis and Mitigation of Oscillations in Inductive Power Transfer Systems with Constant Voltage Load and Pulse Density Modulation", in *Proceedings of the Thirteenth Annual IEEE Energy Conversion Congress and Exposition, ECCE 2021, Vancouver, British Columbia*, Canada / Virtual Conference, 10-14 October 2021, pp. 1565-1572.

[11] M. Fan, L. Shi, Z. Yin, L. Jiang and F. Zhang, "Improved pulse density modulation for semi-bridgeless active rectifier in inductive power transfer system", *IEEE Trans. Power Electron*., vol. 34, no. 6, pp. 5893-5902, Jun. 2019.